A New Single-Cell Measurement Method for Determining the Twist Elastic Constant of Liquid Crystals

Daming Xu, Fenglin Peng, Guanjun Tan, Juan He, Shin-Tson Wu
College of Optics and Photonics, University of Central Florida, Orlando, FL 32816, USA

Abstract
A semi-empirical equation is developed to characterize the optical decay time of in-plane switching (IPS) and fringe field switching (FFS) liquid crystal displays. Good agreement between simulation and experiment is obtained. Moreover, this equation provides a simple yet accurate method to measure the twist elastic constant K_{22} of liquid crystals.

Author Keywords
Liquid crystal; twist elastic constant; measurement

1. Introduction

Liquid crystal displays (LCDs) [1-3] are playing a significant role in our daily lives nowadays. Three widely used LC modes are twisted nematic (TN) [4], vertical alignment (VA) [5], and in-plane switching (IPS) [6] including fringe field switching (FFS) [7]. In TN and VA modes, the longitudinal electric field is uniform so that their dynamic response can be solved analytically [8]. In contrast, the fringing field is non-uniform in IPS and FFS modes [9], thus it is extremely complicated to obtain an analytical solution to describe the response time. Usually, the optical decay time (τ_d) of IPS and FFS modes is assumed to be analogous to those of homogeneous (splay K_{11}) and VA (bend K_{33}) cells [10]:

$$\tau_d \sim \tau_0 = \frac{\gamma_1 d^2}{K_{22}\pi^2}, \quad (1)$$

where γ_1 is the rotational viscosity, d is the cell gap, and K_{22} is the twist elastic constant. Qualitatively, the decay time is indeed proportional to γ_1/K_{22} and d^2, but quantitatively the error is about 25-30%, as will be shown later.

The accurate measurement of K_{22} remains a critical challenge in LC material characterization. Although several simple methods for measuring K_{11} and K_{33} have been developed [11], the methods for determining K_{22} require much more complicated experimental setups or elaborated fitting routine [12-15]. In particular, some methods require two cells for measuring K_{22}. Thus, a simple yet accurate single-cell method to measure K_{22} is urgently needed.

In this paper, we develop a semi-empirical equation to calculate the decay time of IPS cells based on simulations. The model is confirmed by experiment. Next, we apply this simple equation to measure the K_{22} of LC materials. The measured results of 5CB at different temperatures agree well with literature values. Thus, this semi-empirical equation can be used to describe the response time of IPS and FFS cells and it provides a simple yet accurate method to measure the twist elastic constant of LC mixtures.

2. Simulation Results

The dynamic decay processes of both IPS and FFS modes are simulated by TechWiz LCD, a very reliable simulator compared to experiments. In simulations, we investigate IPS and FFS cells with various electrode width (W) and gap (G), such as IPS-5/5 (W = G = 5μm), FFS-2/3 (W = 2μm, G = 3μm), etc. The alignment layer is 80-nm thick polyimide, and the passivation layer in FFS cell is 150-nm Si_3N_4 (ε = 7.5). The physical properties of LC materials studied are listed in TABLE I. Here, HAI (HAI-653265, HCCH, China), DIC-LC2 (DIC, Japan) and ZLI-1132 (Merck, Germany) are positive (+Δε) LCs; while HAV (HAV-634117, HCCH), MX-40593 (LC Vision, USA), and MLC-6882 (Merck) are negative (−Δε) LCs [16]. The K_{22} values of three positive LCs are provided by the vendors, whereas those of the three negative LCs are unknown and need to be measured.

Table I. Physical properties of the six LC mixtures studied (T = 23°C, λ = 633nm and f = 1 kHz).

LC	T_C (°C)	Δε	Δn	γ_1 (m·Pas)	K_{22} (pN)
HAI	80.0	2.4	0.096	42.8	7.8
DIC-LC2	75.5	1.7	0.117	32.0	6.5
ZLI-1132	71.0	12.0	0.137	159.8	6.3
HAV	89.5	-3.79	0.108	98.5	-
MX-40593	79.3	-2.47	0.101	64.4	-
MLC-6882	69.0	-3.1	0.097	108.0	-

(a) Elastic constant effect

We investigate the elastic constant effect by varying each elastic constant within a reasonable range (K_{11} & K_{33}: 5-17 pN, K_{22}: 3-12 pN) while keeping all other material parameters unchanged. The homogeneous rubbing angle is set at 80° or 10° w.r.t. the stripe electrodes axis for IPS or FFS cell using a negative (called n-IPS and p-FFS) or a positive LC (called p-IPS and p-FFS), respectively. Strong anchoring (W=10^{-3} J/m^2) is assumed to all LC cells. Each cell is first biased at its on-state voltage, then the voltage is removed and the decay time for 90% to 10% transmittance change is calculated.

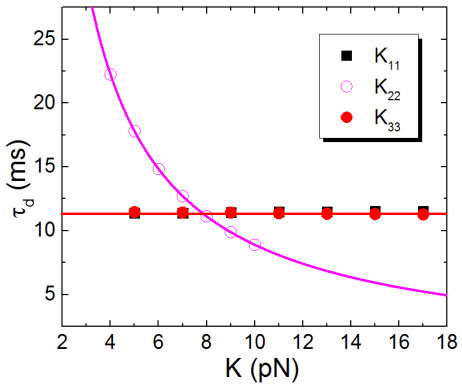

Figure 1. Dependence of decay time on three elastic constants for the IPS-5/5 cell (LC mixture: HAI).

Figure 1 depicts the dependence of τ_d on each elastic constant for the IPS-5/5 cell. Due to the limitation of space, here we only

 ISSN 0097-966X/16/4703-1674-$1.00 © 2016 SID

show the simulation results of p-IPS cell, but the n-IPS and FFS cells exhibit the same trend. It shows that τ_d is independent of K_{11} and K_{33} although the tilt angles are fairly large in p-IPS and p-FFS cells. This is because the tilt angles don't contribute to the transmittance; thus the relaxation of tilted LC directors is not explicitly manifested by the transmittance change during the decay process. In contrast, a different trend is found for the twist elastic constant: τ_d decreases dramatically as K_{22} increases. The reciprocal function is used to fit the simulation results, and good agreement is obtained, as shown in Fig. 1. Hence, the dependence of τ_d on the elastic constants follows:

$$\tau_d \sim 1/K_{22}. \quad (2)$$

(b) Cell gap effect

The cell gap (d) effect is studied by varying d from 2.5 μm to 4.0 μm, and the simulated results are plotted in Fig. 2. To describe the trend, we use a linear function to fit the results, as plotted by the magenta line, and obtain a good agreement. Thus, the dependence of τ_d on the cell gap can be written as:

$$\tau_d \sim d^2. \quad (3)$$

Hence, we can write the decay time as:

$$\tau_d = A \cdot \frac{\gamma_1 d^2}{K_{22}\pi^2}, \quad (4)$$

where A is the slope of the fitting curve. Meanwhile, Fig. 2 shows that A is independent of electrode dimension, indicating that A may only depend on other cell parameters (e.g. rubbing angle) or LC material properties.

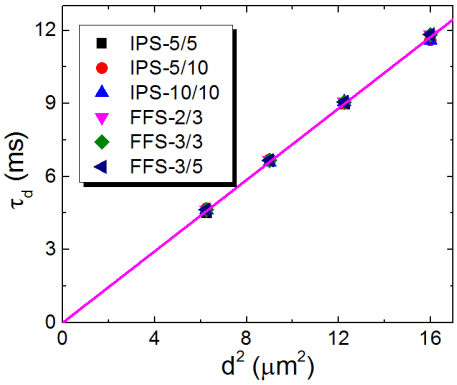

Figure 2. Dependence of decay time on the cell gap for various p-IPS and p-FFS cells (LC: HAI).

(c) LC material dependence

The LC material dependence of A is studied by employing different materials from Table I. Based on each LC, K_{22} is varied within a reasonable range (4-8 pN). Table II compares the A values of the p-IPS cells using three positive LCs. It shows that A is independent of K_{22} and their A values are all in the range of 1.287 ± 0.007 (error: ± 0.54%). Hence, A is independent of LC material properties. This is an attractive feature, as it means that Eq. (4) is universally applicable to all IPS and FFS cells no matter what LC material is employed.

TABLE II. Simulated A values for p-IPS cells employing different LC mixtures.

K_{22} (pN)	HAI	DIC-LC2	ZLI-1132
4	1.289	1.288	1.286
5	1.288	1.280	1.287
6	1.288	1.284	1.285
7	1.291	1.286	1.290
8	1.292	1.284	1.294

(d) Rubbing angle effect

The typical rubbing angle φ_0 is 80° and 10° for -Δε and +Δε LCs, but can vary in the range of φ_0±4° [17]. In our studies, we simulate the A values for p-IPS and n-IPS cells with rubbing angle φ varying in an even wider range (φ_0 ± 8°), as listed in Table III. As rubbing angle φ varies, A remains almost unchanged, which is different from rise time. Taking p-IPS cell as an example, as φ decreases, the rise time becomes slower due to reduced torque on LC directors exerted by the electric field. At the full-bright state, the twist angle should occur at ~φ +45° in order to obtain maximum phase retardation [7]. Hence, although rubbing angles are different, the deviation of LC directors from rubbing angle is almost the same. Upon removal of the voltage, the relaxation torque exerted by surface anchoring remains almost the same. Consequently, the decay time is nearly the same for all these cells and A is not affected by the rubbing angles.

Table III. Simulated A values for p- and n-IPS -5/5 cells employing HAI and MLC-6882, respectively.

φ - φ_0	p-IPS	n-IPS
-8°	1.284	1.281
-4°	1.286	1.286
0°	1.288	1.287
4°	1.289	1.292
8°	1.291	1.289

(e) Anchoring energy effect

In liquid crystal devices, various anchoring conditions W can be used: strong ($W \geq 10^{-3}$ J/m^2), weak ($W \leq 10^{-5}$ J/m^2) and medium anchoring. An important parameter describing the anchoring energy is the extrapolation length given by $L \sim K/W$ [18], which is the distance from the real surface where the LC director would coincide with the original "easy axis" orientation. It can be interpreted as the extension of the LC cell gap:

$$d' = d + 2L. \quad (5)$$

Then Eq. (4) can be further modified to:

$$\tau_d = A_0 \cdot \frac{\gamma_1}{K_{22}\pi^2} \cdot (d+2L)^2 = A_0 \cdot \frac{\gamma_1}{K_{22}\pi^2} \cdot \left(d^2 + \frac{4dK_{22}}{W} + \frac{4K_{22}^2}{W^2} \right), \quad (6)$$

where A_0 is proportionality constant under the infinity anchoring ($W = \infty$). For a medium or weak anchoring, $2K_{22}/W$ is not negligible and we have to consider the anchoring energy term.

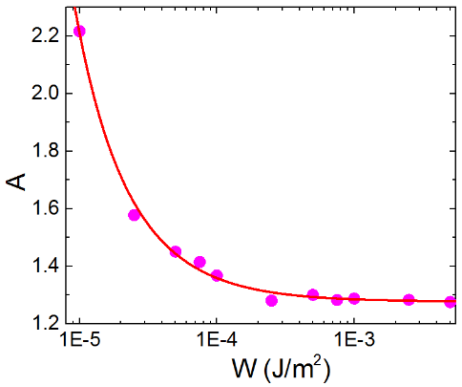

Figure 3. Dependence of A on the anchoring energy for p-IPS-5/5 cell (Rubbing angle φ = 80°, LC: HAI).

To validate these derivations, we simulate the decay time of p-IPS cell under different anchoring conditions. The calculated A values are plotted as magenta dots in Fig. 3, and they are fitted with following equation:

$$A = A_0 \cdot \left(d^2 + \frac{4dK_{22}}{W} + \frac{4K_{22}^2}{W^2} \right). \quad (7)$$

The fitting results are plotted as the red line, and it well aggress with the discrete dots. Therefore, Eqs. (6) and (7) well describe the anchoring energy effects in IPS cells. The proportionality constant under infinity anchoring ($W = \infty$) is A_0 = 1.277. Next, we will validate this in experiments.

3. Experimental Results

(a) Experiment vs. Simulation

In experiments, we prepare three IPS-10/10 cells with strong anchoring energy using the positive LCs listed in Table I. We measure the transient transmittance decay process from the full-bright to dark state with a digital oscilloscope, and the measured optical decay times are included in Table IV. Based on material properties, we also calculated the proportionality constant A, as also shown in Table IV. We find that A is in the range of 1.238 ± 0.016 (error: ±1.29%). Compared to the simulated value (A = 1.287), the experimental value is 3.41% lower, which is acceptable considering the discrepancy between simulation and experiment. Hence, our experiment validates that there is indeed a non-unity proportionality constant A that is universally applicable to describe the optical decay time of IPS cells:

$$\tau_d = 1.238 \cdot \frac{\gamma d^2}{K_{22}\pi^2}. \quad (8)$$

TABLE IV. Measured cell gap, optical decay time and A values for three IPS-10/10 cells. (T = 23°C, λ = 633nm).

LC	d (μm)	τ_0 (ms)	τ_d (ms)	A
HAI	3.71	7.65	9.35	1.222
DIC-LC2	3.23	5.20	6.47	1.244
ZLI-1132	3.69	34.99	43.88	1.254

(b) 5CB Measurement

To further verify the applicability of Eq. (8), we measure the K_{22} values of the well-studied 5CB under different temperatures and then compared our data with published results. We inject 5CB into an IPS-10/10 cell and measured the decay time at different temperatures. Then the temperature-dependent K_{22} values were calculated using Eq. (8), as depicted as the blue diamonds in Fig. 4. For comparison purpose, we also include the measured data by Breddels (magnetic field measurement method) [19] and Hara [20]. It clearly shows that our measured data agrees well with literature results, thus proving that Eq. (8) is indeed accurate.

The K_{22} values measured by our method are further verified by order parameter $\boldsymbol{S}$, which can be described by:

$$S = \left(1 - T / T_C\right)^{\beta}. \quad (9)$$

Here, T_C is the clearing point of the LC material and β is a material constant. The order parameter affects the physical properties of LC material, e.g. birefringence Δn and elastic constant K_{ii} are related to order parameter by:

$$\Delta n = \Delta n_0 \cdot S, \quad (10)$$

$$K_{ii} = c_i \cdot S^2, \quad (11)$$

where Δn_0 and c_i are the extrapolated birefringence and elastic constant at T = 0K.

In experiment, we also measured the Δn of 5CB at different temperatures. The temperature-dependent birefringence was then fitted with Eq. (9)-(10). We obtained T_C = 308.3 K and β = 0.142, consistent with prior literature [21]. Then we plotted the measured K_{11} and K_{22} as functions of S^2, as shown in Fig. 5. We fitted the measured data with Eq. (11), and obtained a very good agreement, indicating that our measurement method is reliable. Here, the fitting parameters are c_1 = 17.45 pN and c_2 = 9.10 pN.

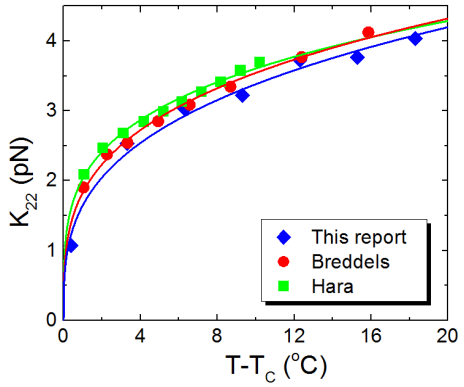

Figure 4. Temperature-dependent K_{22} values of 5CB.

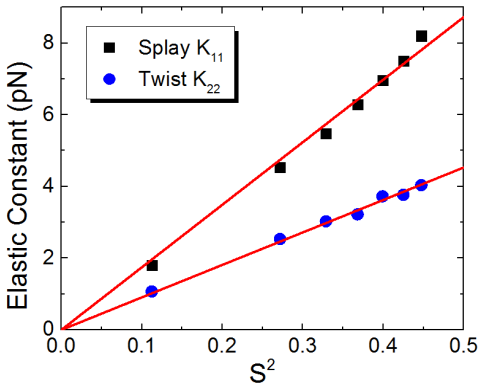

Figure 5. K_{11} and K_{22} of 5CB as a function of order parameter.

(c) Material development

Recently, extensive efforts have been devoted to achieve faster response time for IPS and FFS LCDs, including device designs

[22-24] and material development. Among them, lowering visco-elastic coefficient γ_1/K_{22} is a very effective method from the material side. Since γ_1 can be measured very easily, low-viscosity materials are well studied in material designs [25, 26]. In contrast, due to the difficulties in K_{22} measurement, the impact of K_{22} is sometimes overlooked. Now, with the verified semi-empirical equation presented above, we are able to accurately evaluate the visco-elastic coefficient for IPS and FFS LC materials.

We first measured the K_{22} values of the negative materials listed in Table I. Their K_{22} values were found to be 6.4 pN (HAV), 5.4 pN (MX-40593) and 7.9 pN (MLC-6882), respectively. To compare their performance, we plot their visco-elastic coefficient γ_1/K_{22} in Fig. 6, as shown by the magenta squares. Here, two other negative LC materials with higher dielectric anisotropy from Merck, namely MLC-6608 ($\Delta\varepsilon$ = –4.2) and MLC-6609 ($\Delta\varepsilon$ = –3.7), are also measured and their γ_1/K_{22} values are found to be 18.87 and 18.32 ms/μm2, respectively. Meanwhile, we also plot the γ_1/K_{22} values for various positive LCs with the blue dots. All the measured materials have Δn ~ 0.1 and clearing point around 80°C, which is intended for practical applications.

From Fig. 6, for both positive and negative LCs, as $\Delta\varepsilon$ decreases (fewer polar component) γ_1/K_{22} gets smaller as well, leading to a faster response time. But the tradeoff is increased voltage. Therefore, a delicate balance between response time and operation voltage has to be taken into account simultaneously for material design. The optimal $|\Delta\varepsilon|$ value depends on the intended operation voltage. For both IPS and FFS modes, the strategy is to use a minimally acceptable $|\Delta\varepsilon|$ in order to take advantages of small visco-elastic coefficient.

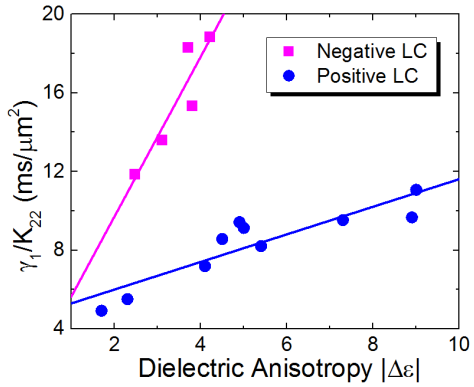

Figure 6. Visco-elastic coefficient vs. $|\Delta\varepsilon|$ of some LC mixtures with Δn ~ 0.1 and clearing point around 80°C.

4. Conclusion

We have developed a simple yet accurate semi-empirical equation to describe the optical decay time of IPS and FFS modes. It serves two important objectives: 1) it reliably describes the optical response time of IPS and FFS cells, and 2) it provides a simple single-cell method to measure the twist elastic constant accurately.

5. Acknowledgments

The authors are indebted to AU Optronics (Taiwan) and AFOSR for the financial supports under contract No. FA9550-14-1-0279.

6. References

[1] M. Schadt, "Milestone in the history of field-effect liquid crystal displays and materials," Jpn. J. Appl. Phys. **48**, 03B001 (2009).
[2] Z. Luo, D. Xu, S. T. Wu, "Emerging quantum-dot-enhanced LCDs," J. Disp. Technol. **10**, 526-539 (2014).
[3] D. Franklin, Y. Chen, A. Vazquez-Guardado, S. Modak, J. Boroumand, D. Xu, S. T. Wu, D. Chanda, "Polarization-independent actively tunable color generation on imprinted plasmonic surfaces," Nature Commun. **6**, 7337 (2015).
[4] M. Schadt, W. Helfrich, "Voltage-dependent optical activity of a twisted nematic liquid crystal," Appl. Phys. Lett. **18**, 127 (1971).
[5] M. F. Schiekel, K. Fahrenschon, "Deformation of nematic liquid crystals with vertical orientation in electrical fields," Appl. Phys. Lett. **19**, 391 (1971).
[6] M. Oh-e, K. Kondo, "Electro-optical characteristics and switching behavior of the in-plane switching mode," Appl. Phys. Lett. **67**, 3895 (1995).
[7] S. H. Lee, S. L. Lee, H. Y. Kim, "Electro-optic characteristics and switching principle of a nematic liquid crystal cell controlled by fringe-field switching," Appl. Phys. Lett. **73**, 2881 (1998).
[8] P. Pieranski, F. Brochard, E. Guyon, "Static and dynamic behavior of a nematic liquid crystal in a magnetic field. Part II: Dynamics," J. Phys. **34**, 35 (1973).
[9] D. Xu, F. Peng, H. Chen, J. Yuan, S. T. Wu, M. C. Li, S. L. Lee, W. C. Tsai. "Image sticking in liquid crystal displays with lateral electric fields," J. Appl. Phys. **116**, 193102 (2014).
[10] H. Wang, T. X. Wu, X. Y. Zhu, S. T. Wu, "Correlations between liquid crystal director reorientation and optical response time of a homeotropic cell," J. Appl. Phys. 95, 5502 (2004).
[11] H. Gruler, T. J. Scheffer, and G. Meier, "Elastic constants of nematic liquid crystals," Z. Naturforsch **27a**, 966 (1972).
[12] P. R. Gerber, M. Schadt, "On the measurement of elastic constants in nematic liquid crystals: comparison of different methods," Z. Naturforsch. **35a**, 1036 (1980).
[13] S. Faetti, M. Gatti, V. Palleschi, "A new torsion pendulum technique to measure the twist elastic constant of liquid crystals," J. Phys., Lett. **46**, L881 (1985).
[14] F. M. Leslie, C. M. Waters, "Light scattering from a nematic liquid crystal in the presence of an electric field," Mol. Cryst. Liq. Cryst. **123**, 101 (1985).
[15] E. P. Raynes, C. V. Brown, J. F. Stromer, "Method for the measurement of the K_{22} nematic elastic constant," Appl. Phys. Lett. 82, 13 (2003)
[16] D. Xu, F. Peng, G. Tan, J. He, S. T. Wu, "A semi-empirical equation for the response time of in-plane switching liquid crystal display and measurement of twist elastic constant," J. Appl. Phys. **117**, 203103 (2015).
[17] J. H. Lee, D. J. Lee, S. W. Oh, M. K. Park, K. H. Park, B. K. Kim, H. R. Kim, "Viewing-angle property of single-domain AH-IPS liquid-crystal mode optimized with polymer-stabilized polystyrene alignment layer," SID Int. Symp. Digest **45**, 314 (2014).
[18] X. Nie, R. Lu, H. Xianyu, T. X. Wu, S. T. Wu, "Anchoring energy and cell gap effects on liquid crystal response time," J. Appl. Phys. **101**, 103110 (2007).
[19] P. A. Breddels, J. C. H. Mulkens, "The Determination of the Frank elastic constant for twist deformation of 5CB using a conoscope," Mol. Cryst. Liq. Cryst. **147**, 107 (1987).
[20] M. Hara, J. I. Hirakata, T. Toyooka, H. Takezoe, A. Fukuda, "Determination of the Frank elastic constant ratios in nematic liquid crystals (nCB) by observing angular dependence of rayleigh light scattering intensity," Mol. Cryst. Liq. Cryst. **122**, 161 (1985).
[21] J. Li, S. T. Wu, "Extended Cauchy equations for the refractive indices of liquid crystals," J. Appl. Phys. **95**, 896 (2004).

[22] D. Xu, L. Rao, C. D. Tu, S. T. Wu, "Nematic liquid crystal display with submillisecond grayscale response time," J. Disp. Technol. **9**, 67-70 (2013).
[23] D. Xu, H. Chen, S. T. Wu, M. C. Li, S. L. Lee, W. C. Tsai, "A fringe field switching liquid crystal display with fast grayscale response time," J. Disp. Technol. **11**, 353-359 (2015).
[24] H. Chen, Z. Luo, D. Xu, F. Peng, S. T. Wu, M. C. Li, S. L. Lee, W. C. Tsai, "A fast-response A-film-enhanced fringe field switching liquid crystal displays," Liq. Cryst. **42**, 537-542 (2015).
[25] H. Chen, F. Peng, Z. Luo, D. Xu, S. T. Wu, M. C. Li, S. L. Lee, W. C. Tsai, "High performance liquid crystal displays with a low dielectric constant material," Opt. Mater. Express **4**, 2262 (2014).
[26] H. Chen, M. Hu, F. Peng, J. Li, Z. An, S. T. Wu, "Ultra-low viscosity liquid crystals," Opt. Mater. Express **5**, 655 (2015).